Over a hundred years later, the classic antenna, first invented by Heinrich Hertz, in 1888, [1], is still the dominant technology used for the measurement of RF fields. Just seven years after its invention, Guglielmo Marconi applied the antenna to long-distance radio communication and, in the process, transformed the global community into one connected civilization [2]. It is clear that the antenna has been a powerful piece of technology. What reason would we have, then, to use anything different?

In fact, researchers around the world are developing a new atomic RF receiver that has the potential to either replace or work in tandem with traditional antennas in a variety of applications. While most antennas, based on their geometries, detect a limited bandwidth of frequencies, these new atomic receivers are tunable over a very wide range of frequencies, from megahertz to terahertz, without changes to any of the hardware. This enables ultra-wideband detection with a single receiver. In environments where a receiver is hard to reach (on a satellite, for example) and where space limitations mean that arrays of antennas are impossible, a receiver with programmable frequency tuning over an extremely wide range of frequencies may prove to be quite valuable.

Modern RF Measurements With Hot Atoms

Alexandra Artusio-Glimpse (alexandra.artusio-glimpse@nist.gov), Matthew T. Simons (matthew.simons@nist.gov), Nikunjkumar Prajapati (nikunjkumar.prajapati@nist.gov), and Christopher L. Holloway (christopher.holloway@nist.gov) are with the National Institute of Standards and Technology, Boulder, Colorado, 80305, USA.

Digital Object Identifier 10.1109/MMM.2022.3148705

Date of current version: 4 April 2022

IMAGE LICENSED BY INGRAM PUBLISHING

Researchers around the world are developing a new atomic RF receiver that has the potential to either replace or work in tandem with traditional antennas.

Another major difference of these atomic receivers as compared to traditional antennas involves the sensing head. The atomic receiver detects changes in the susceptibility of a glass cell containing a single species of atoms in vapor (many more details on how these receivers work are given later in this article). No metal material is needed to detect RF electric (E) fields. Changes to the susceptibility of the atomic vapor are measured as variations in the transmitted power of a probe laser. An RF antenna that is made of glass and atomic vapor, as opposed to bulk metal, is going to have lower material losses. Furthermore, the glass receiver is likely to scatter less of the incident RF radiation and may be advantageous in stealth applications where the receiver's location and the received signal need to be protected from eavesdropping adversaries.

A third asset of the atomic receiver is its direct link to the International System of Units (SI) [3], [4]. Antennas that operate at bands above 100 GHz are challenging to reliably calibrate. Currently, an absolute standard for calibration at these frequencies does not exist. Designing new receivers for millimeter-wave fields is a major focus of metrologists and engineers, and novel solutions to the challenges presented by the classic antenna are required. Atomic RF receivers are a promising solution to this need for absolute field calibrations above 100 GHz because the atomic response to high-frequency fields is knowable based on the atomic energy states, leaving only the effects of the vapor cell to be calibrated.

In this article, we look at this new RF E-field receiver and its potential in RF communications, sensing, and metrology. Since the development of single-frequency, visible lasers that can be stably tuned over a range of several terahertz, atomic RF E-field sensors operating at room temperature (0–40° C) have become the focus of considerable research [5], [6], [63]. Not only can we measure the strength of an incident RF E-field with atom-based sensors, we can also detect the phase and tune the polarization response. This means that devices such as the one pictured in Figure 1 could replace the classic antenna in precision metrology, communications, and a variety of other sensing applications.

How We Measure E-Fields With Atoms

Room temperature vapor consisting of a single species of alkali atoms, our "hot atoms," is at the center of this new receiver technology. Alkali metals, such as rubidium and cesium, have a single electron in the outermost orbital. Through optical excitation, we can drive this electron into an energy state with a high principle

Alexandra Artusio-Glimpse, Matthew T. Simons, Nikunjkumar Prajapati, and Christopher L. Holloway

quantum number (e.g., $n > 20$), a so-called Rydberg state [8]. A higher principle quantum number means that the electron is farther from the nucleus, where the radius of the new orbit scales with n^2. Far from the nucleus, with the core electrons effectively shielding the positive nuclear charge, the valance electron is loosely bound and highly sensitive to perturbations from incident electric and magnetic fields. The binding energy, in fact, scales as $1/n^2$. In this way, we can detect an incident RF E-field with loosely bound electrons in a dielectric chamber of alkali vapor.

A single Rydberg sensor is easily tunable from megahertz to terahertz frequencies [9], [10] because its sensitivity band is defined by the frequency of the lasers that excite the atoms into the desired Rydberg state, which are themselves broadly tunable. Therefore, without changing any of the hardware, the Rydberg sensor can be made sensitive to a number of radio frequencies within a wide range. In its simplest form, the response of the Rydberg sensor to the strength of an incident E-field scales as $\wp/h$, where $\wp$ is the dipole moment of the associated atomic transition and h is Planck's constant [5], [6]. With proper selection of the Rydberg states [9], [10], the Rydberg sensor can easily detect frequencies over 100 GHz [9], [11], [12]. What is more, these atomic dipole moments are well-defined by atomic theory, do not change with environmental conditions, and can be calculated with better than 1% accuracy [8]. This means that the RF field measurements depend on a fixed property of the alkali atom, known from well established theory, and Planck's constant, a fundamental quantity ($6.62607015 \times 10^{-34}$ J Hz^{-1}) in the new SI [3], [4]. This results in an SI traceable measurement of RF E-fields that can be used as a sensor and communications receiver.

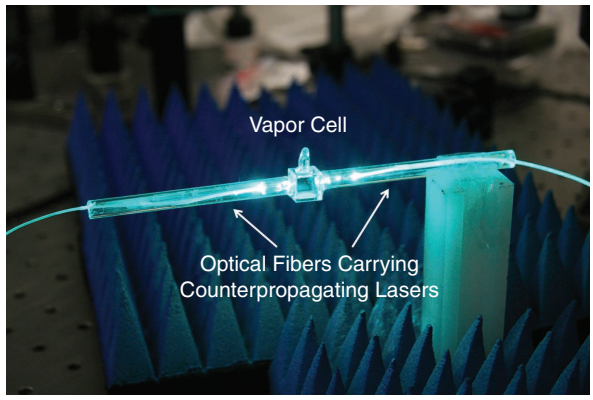

Figure 1. *The Rydberg atom sensor for RF E-field measurements. Here, a 10-mm^3 vapor cell is connected to optical fibers carrying two lasers for targeting specific Rydberg atomic states that are sensitive to an RF signal of interest. See [7] for details of the fiber-coupled sensor.*

As mentioned, Rydberg states are generated with a set of lasers. The frequency of each laser is resonant with specific energy transitions of the alkali atoms that are used. A common system uses two lasers in a ladder design, as depicted in Figure 2. In this architecture, a near-infrared probe laser is resonant with a ground transition of the atom and is absorbed. The amount of absorption is monitored with a photodetector placed after the vapor cell. As we tune the frequency of the probe laser away from resonance with the ground transition, we see decreased absorption of the laser by the atomic vapor. The width of this absorption line is dictated by the velocity of the room temperature atoms moving relative to the laser photons, resulting in Doppler broadening of the resonant line; this Doppler-broadened probe absorption is shown in Figure 3 as the red curve.

When we introduce a higher-energy (i.e., a visible wavelength) laser, we induce a narrow window of transparency that comes from the interference of two excited states—the state reached with the probe laser and that reached with the visible laser, called the *coupling laser*. The effect is known as *electromagnetically induced transparency*

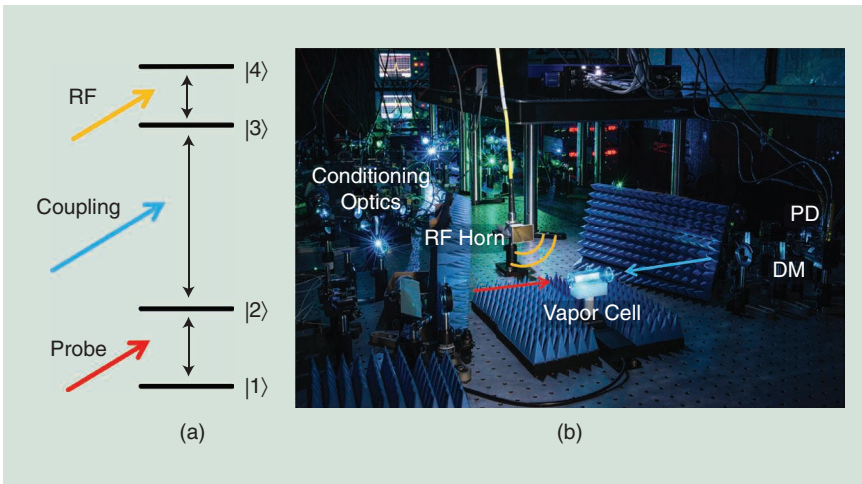

Figure 2. *A vapor cell of alkali atoms, for example, Rubidium-85, is excited from the ground state $|1\rangle$ by a set of lasers (the probe and coupling lasers) to a Rydberg state $|3\rangle$ that is then coupled to a neighboring Rydberg state $|4\rangle$ by an RF field. (a) A basic ladder scheme; other schemes with three or more lasers can be used. (b) The system in the lab, with a photodetector (PD) for capturing the transmitted power of the probe laser through the vapor cell and a dichroic mirror (DM) that passes the probe light and reflects the coupling light.*

(*EIT*) [13], [14]. The coupling laser drives the atoms into the Rydberg state, where the valance electron is only weakly bound to the nucleus. Under this condition, the atoms are now sensitive to low-energy E-fields. The EIT line, depicted in Figure 3 as the blue curve, undergoes splitting due to the Autler–Townes (AT) effect when the atoms are exposed to the RF radiation. This splitting is illustrated in Figure 3 as the yellow curve. The difference in frequency between the two newly formed transmission windows is directly proportional to the magnitude of the incident RF E-field through the relationship $\Delta_f = \wp |E_{\mathrm{RF}}|/h$.

Rydberg sensors are being developed as an absolute standard for the calibration of antennas and other devices that require known RF E-field strengths, due to the direct link to the SI and atomic behavior as described by quantum mechanics [6], [9]–[11]. In these systems, the coupling laser frequency is judiciously chosen such that the RF field of interest is resonant with a nearby Rydberg state, and AT splitting occurs. This measurement of E-field magnitude is absolute and directly linked to the SI. Below, we also look at relative measurements that can be used to determine the phase and polarization of the E-field.

Several groups have started looking into measurement uncertainties associated with Rydberg sensors [6], [15], [16]. So far, they have found that two factors dominate uncertainty in the field strength measurements of RF E-fields. The first is laser intensity detection noise. This statistical source of uncertainty impacts the frequency measurement of the AT splitting and is estimated to contribute approximately 0.5% relative uncertainty to the measurement of the AT splitting frequency [6], [16]. The second source comes from the dielectric vapor cell containing the alkali atoms, which causes perturbations of the RF E-field inside the cell. These perturbations can be either modeled or measured and impart roughly 0.5% relative uncertainty to the field strength measurement with standard vapor cells [12], [16], [17].

Smaller sources of uncertainty include the calibration of the measured frequency scale (~0.06% [16]), calculation of the dipole momentum (~0.1% [18]), and deviations from linearity in the relationship between the amount of splitting and the strength of the field being measured [15]. At low field strengths, techniques such as heterodyning significantly enhance the sensitivity of the measurement [19], and have different linear conditions than AT splitting. On the other hand, very strong fields cause the AT splitting to leave the linear regime, due to the very large frequency shifts caused by the ac Stark effect, which scale as the field strength squares [20], [21]. AC Stark shifts also come into effect when the RF field is off resonance with the atoms. In this regime, the splitting frequency may not be linear, but it is well characterized by more complex models [22].

The glass receiver is likely to scatter less of the incident RF radiation and may be advantageous in stealth applications where the receiver's location and the received signal need to be protected.

Additionally, external sources of electric and magnetic fields (e.g., Earth's magnetic field) can contribute to the systematic uncertainty in the RF E-field strength measurement if the atoms are not sufficiently shielded [6].

The probe transmission signal in Rydberg atom sensors is dependent on the dot products of the E-fields of the probe laser, coupling laser, and RF field [23]. Thus, by understanding this dependence, a vector field electrometer can be implemented. Such a system has been demonstrated with a linear polarization angular resolution of 0.5% [23]. In this setup, the atomic transitions define the field polarization response of the sensor, given a particular polarization orientation of the two laser fields [Figure 4(a)]. Alternatively, one can also place the vapor cell inside a polarization-selective antenna [24], [25], [Figure 4(b)], which offers additional opportunities, such as using a field-enhancing resonator and applying a local oscillator (LO) across the antenna for sensitivity enhancement and phase detection.

To detect the phase of an incident RF field, the RF signal must be compared to a known reference. There

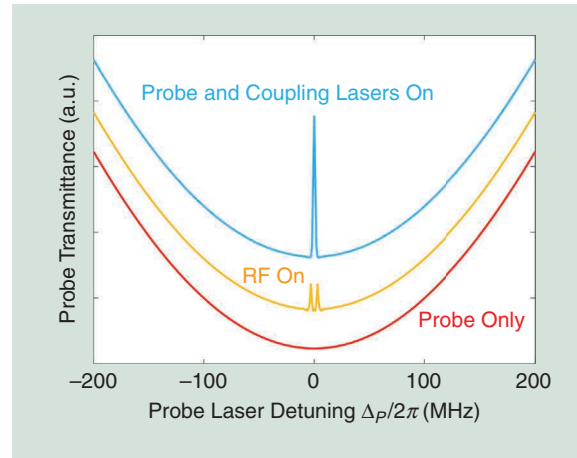

Figure 3. *The electromagnetically induced transparency signal as the probe laser is detuned from resonance, showing the wide Doppler background of the probe absorption line. When the coupling laser is added, a narrow transmission window appears and splits into two transmission peaks upon exposure of the atoms to the RF field (so-called Autler–Townes splitting). These curves have been shifted vertically with respect to one another for better visibility.*

Designing new receivers for millimeter-wave fields is a major focus of metrologists and engineers, and novel solutions to the challenges presented by the classic antenna are required.

are two techniques for doing this. The first applies an RF heterodyne or homodyne principle through an RF LO field [26], [27]. In this case, the atomic receiver acts as both a receiver and a mixer that outputs a down-converted signal at the intermediate frequency (IF) of the LO and signal RF fields. When a heterodyne system is implemented, this down-converted mixer output can be fed into a vector network analyzer or lock-in amplifier to extract in-phase and quadrature or magnitude and phase outputs. Alternatively, when a homodyne system is implemented, the LO is at the same frequency as the signal RF field but with a different phase. A dc signal that depends on the relative phase between the LO and signal RF fields is output from the Rydberg sensor. By tuning the LO phase, one can map the phase response, given a fixed signal field strength, and determine the phase of the signal field, based on the point of constructive interference between the two RF fields. Both the RF heterodyne system and RF homodyne system can take advantage of a polarization-selective antenna near the vapor cell where the antenna is used to apply the LO [25]. Additionally, there is an amplification of the signal RF field when this method is implemented, leading to a strong enhancement of the sensitivity of the atom sensor [19].

The second technique used for determining the phase of an incident RF field employs phase-coherent excitation pathways with the coupling laser [28], [29]. In this all-optical phase sensing approach, the coupling laser is phase, amplitude, or frequency modulated

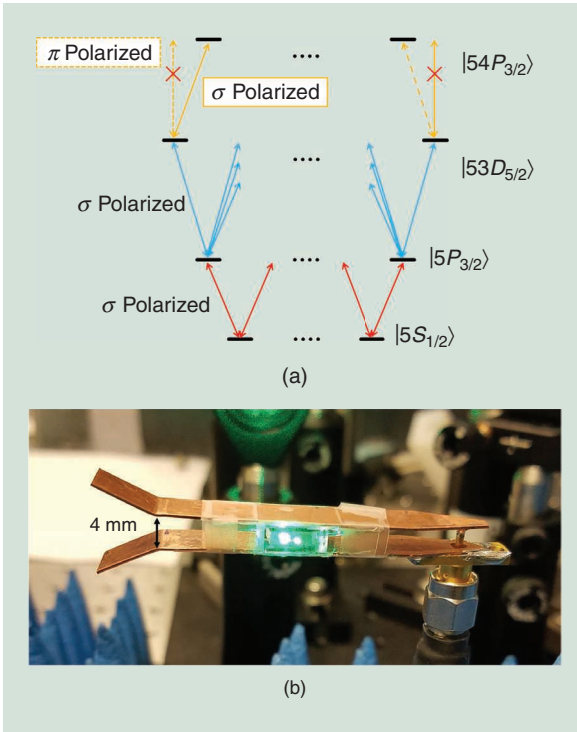

Figure 4. *E-field polarization can be detected by (a) tracing the specific response of the atomic states to differing polarization states (where σ and π denote 3D polarization directions relative to the atoms) [23] and (b) embedding the vapor cell into a polarization-selecting waveguide or resonator.*

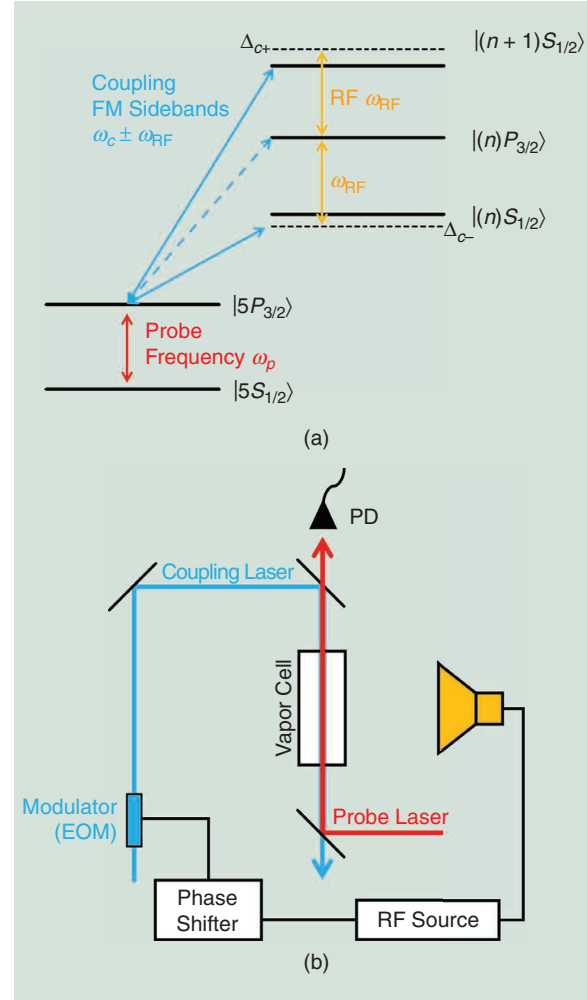

Figure 5. *The (a) level diagram and (b) experimental setup for detecting the phase of an incident RF E-field through the interference of optically addressed atomic states [28]. This all-optical technique differs from an RF heterodyne approach wherein the RF signal is interfered with a second RF source, referred to as an LO. EOM: electrooptic modulator.*

(FM) at an RF via electrooptic modulation, and a phase delay of this field is applied. The RF modulation of the coupling laser should be equal to the frequency of the signal RF field to be measured. This frequency also equals half the separation between two neighboring Rydberg levels. A picture of such a system is in Figure 5. The coupling laser and the incident RF field coherently connect this pair of atomic states along two different paths, creating an atom interferometer. The atom interferometer is sensitive to both the phase and magnitude of the incident RF field. By tuning the phase of the optical photons via the phase shifter, the RF field phase and magnitude can be determined [28], [29].

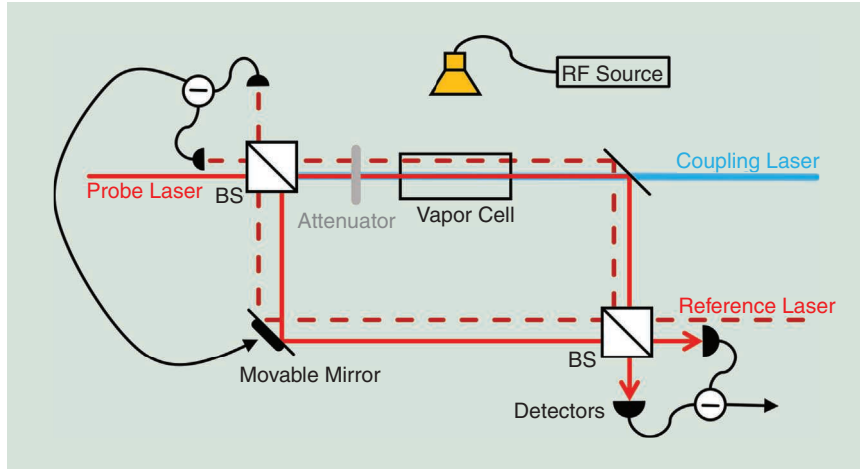

Figure 6. *The optical homodyne setup reduces measurement noise from the probe laser and improves detection sensitivity to RF fields [30]. A Mach–Zehnder interferometer setup is used, with two beam splitters (BS), an attenuator, and a reference laser for optimizing the cavity length with the movable mirror.*

Pushing the Boundaries of Sensitivity and Bandwidth

The standard resonant EIT/AT technique is routinely used to measure E-field strengths down to a few millivolts per centimeter [6], [9], [10], [12], [15]. The sensitivity limit of this measurement is defined by the linewidth of the EIT transmission window, where the RF field-induced AT splitting needs to be on the order of the EIT linewidth to be resolvable. Meanwhile, the bandwidth of this system is defined by the number of resonant Rydberg states that can be reached. Although the neighboring Rydberg states enable a very wide range of resonant frequencies, from hundreds of megahertz to terahertz, there is a fixed number of Rydberg states available, each resonating with a narrow band of E-field frequencies. Recently, researchers have demonstrated several improvements to the standard resonant EIT/AT technique that both increase the sensitivity of the Rydberg sensors and extend the bandwidth of the resonant EIT/AT measurement.

To measure weaker fields, four methods have been put forward. An optical homodyne technique has been demonstrated, showing E-field sensitivities of $5\,\mu\mathrm{V/cm}\sqrt{\mathrm{Hz}}$ [30]. A Mach–Zehnder interferometer with a homodyne detection technique reduces noise from the probe laser and enhances the EIT signal with a strong optical LO; the setup of this system is shown in Figure 6. Such measurements achieved some of the lowest sensitivity with atom receivers until the RF heterodyne technique was introduced. The RF heterodyne, or superheterodyne, technique radiates the atoms with a strong RF LO to enhance sensitivity by reducing noise. In this system, depicted in Figure 7, the Rydberg atoms function as a mixer, down-converting the RF signal to the IF between the signal and the LO fields. This down-converted signal can be easily locked into with a lock-in amplifier. The RF mixer has been shown to achieve an E-field sensitivity of $790\,\mathrm{nV/cm}\sqrt{\mathrm{Hz}}$ while also demonstrating 0.1-Hz frequency discrimination against fields equal in strength to the signal [19]. The sensitivity enhancement of the RF superheterodyne technique can be optimized by setting the LO strength such that the AT splitting due to this field is equal to the full-width half-max of the EIT. Such a system has

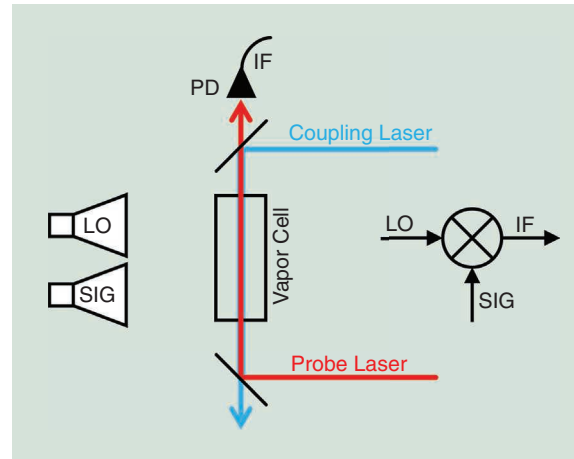

Figure 7. *In the RF heterodyne method, the atoms act as a mixer, and the probe laser transmittance on the PD is a signal at the IF between the LO and signal RF field (SIG). This sensitivity enhancement technique has the added benefit of also being sensitive to phase.*

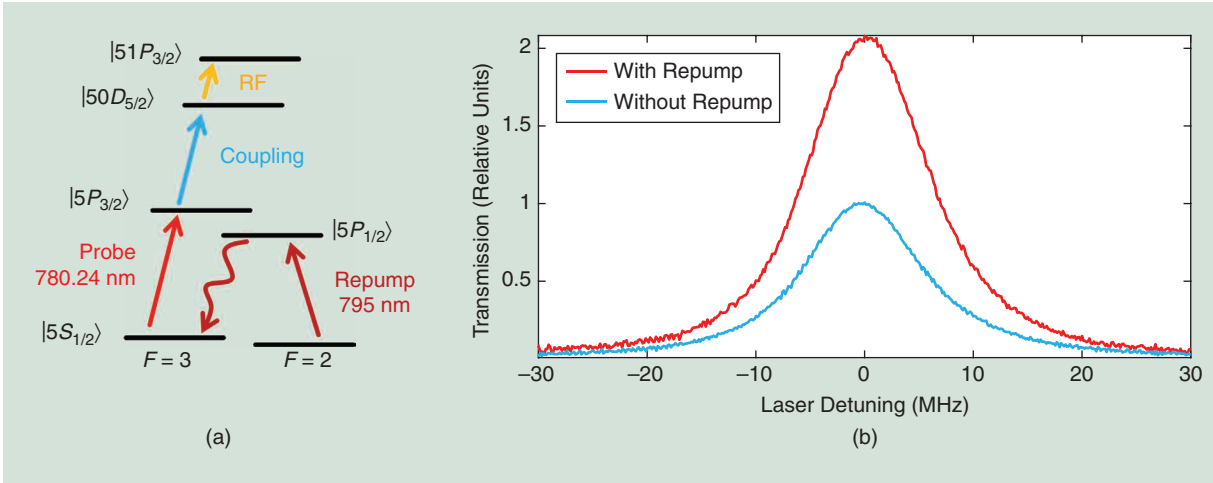

Figure 8. *Atoms populating the $5S_{1/2}$ $F = 2$ state are pumped with a 795-nm laser and decay into the $5S_{1/2}$ $F = 3$ state, where the probe laser (780.24 nm) and coupling laser (480 nm) can excite them into the Rydberg state that is subsequently excited by the RF field. (a) The energy in rubidium. (b) The probe laser transmission as the coupling laser is detuned with and without the repumping (795-nm) laser [32].*

been used to demonstrate E-field root-mean-square sensitivity of 55 $\mathrm{nV/cm}\sqrt{\mathrm{Hz}}$ (or 78 $\mathrm{nV/cm}\sqrt{\mathrm{Hz}}$ peak-to-peak sensitivity) [27]. An RF heterodyne technique can also be implemented when observing the ac Stark effect with strong RF fields. Such a configuration has been used to create an atom-based spectrum analyzer, from dc to 20 GHz [31].

Further improvements to these sensitivity enhancement techniques are possible by repopulating the Rydberg states via a repumping laser. As the electrons in the Rydberg states decay back to ground, not all atoms return to the original ground state targeted with the probe laser. Those atoms whose electron decays to a different state no longer can contribute to the signal unless the electron is repumped into a path that decays back into the targeted ground state. An energy diagram of this repumping technique is given in Figure 8. The detection limit of an RF heterodyne system was recently shown to be reduced by a factor of two through this repumping technique, further improving the sensitivity of the Rydberg sensor to 30 $\mathrm{nV/cm}\sqrt{\mathrm{Hz}}$ [32]. The fourth option for enhancing the sensitivity of Rydberg atom sensors is to use an E-field-confining resonator to enhance the strength of the RF field near the atoms. An example of such a system was demonstrated by Anderson et al. [24]. The team detected ac shifts and reported a 24-dB gain in intensity sensitivity with the split plate resonator. Their embedded resonator device is displayed in Figure 9.

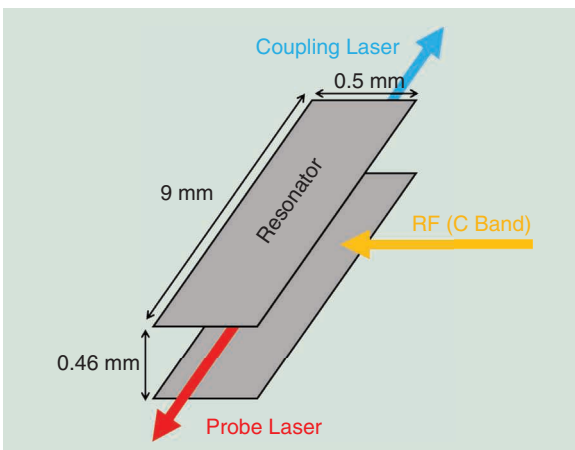

Figure 9. *A split plate resonator embedded in a vapor cell is used for local E-field enhancement near the atoms [24].*

While the range of frequencies that can be detected with a single Rydberg atom E-field-sensing device is exceptionally wide (megahertz to terahertz), only a discrete set of frequencies, each with narrow bandwidth, are detectable with the standard EIT/AT method. The same RF heterodyne technique that enables the measurement of phase and improves measurement sensitivity can also widen the detection bandwidth of these discrete RFs by tuning the LO. However, the best technique shown to achieve continuous frequency sensitivity with Rydberg atom sensors applies a tuning RF field. An adjacent Rydberg resonance tuning field enables EIT/AT detection of very detuned signal fields, resulting in continuous frequency sensitivity [33]. In this way, Rydberg sensors are no longer constrained to detecting a discrete set of RFs. AC Stark shifts can also be used for continuous frequency detection [28], but this approach requires very high field strengths. For weak-field, continuous frequency detection, the method in [33] shows the most promise.

Detecting Modulated Signals for Communication

A huge number of applications rely on time-varying RF signals. These may be amplitude-modulated (AM) signals, FM signals, phase-modulated signals, or combinations, such as quadrature AM (QAM) signals. Rydberg atom sensors are suitable for any of these modulation types, which means they can potentially be used for a wide variety of communications applications. Two regimes exist when detecting AM and FM signals with Rydberg atom sensors [34]. The first applies to weak RF fields with little modulation depth. In this case, the probe laser frequency is locked to the resonant frequency of the ground state transition. As the RF field is modulated, the probe transmission changes at the modulation frequency. No demodulation circuitry is needed because the atoms naturally extract information from the carrier frequency as an amplitude modulation of the probe-transmitted power at the baseband; Figure 10 shows how the probe laser transmittance changes as the RF field is AM or FM for a given Rydberg state, laser power, and RF carrier wave.

Strong RF fields cause AT splitting of the EIT line. In this case, it is necessary to lock the probe laser to a frequency that is tuned away from resonance with the ground state transition. This matches the probe frequency to the AT splitting frequency such that the modulated transmission signal is maximized. Figure 10 also depicts the evolution of the probe transmission for strong fields with amplitude and frequency modulation. An optimal detuning frequency of the probe laser exists and depends on the average strength of the AM/FM field and the linewidth of the EIT. The EIT linewidth is a function of several factors, including the temperature of the atoms, power of the optical lasers (in particular, the probe), width of the optical beams, difference in the frequency of the lasers and their relative propagation directions, number of atoms in the chamber, and principal quantum number of the Rydberg states, as the size of each atom is proportional to n^2, meaning that atoms at higher states are more likely to collide with one another.

Many groups have demonstrated AM and FM measurements with room temperature Rydberg atoms [34]–[39]. The atoms have even been used to detect multiple channels in a musical signal [34], [40]. These groups are studying the effects of noise [34], [41], finding that this detection method is robust even when the signal-to-noise ratio is low. They are also learning that the modulation frequency bandwidth of these sensors is limited by the lifetimes of the first excited state. The cutoff modulation frequency is generally on the order of 1–10 MHz when using Rydberg atom sensors [35], [36], [39], [42]. Increasing the data capacity of a given Rydberg sensor is also possible by passing an array of lasers through the vapor cell and using the signals in combination [43].

As discussed, the phase of an RF field can be detected with Rydberg atom sensors. Using those techniques, we can detect phase-modulated signals, such as binary phase-shift keying (BPSK), quadrature phase-shift keying (QPSK), and quadrature amplitude modulation. Using a vector signal analyzer, Holloway et al. demonstrated the reception of BPSK, QPSK, 16-QAM, 32-QAM, and 64-QAM signals with a symbol rate of 100 kSym/s and error rates below 5×10^{-2} [42]. They also found that symbol rates up to 1 MSym/s can be detected with less than 1×10^{-1} error. They noted that higher symbol rates can also be detected but at the cost of significantly increased error rates. When

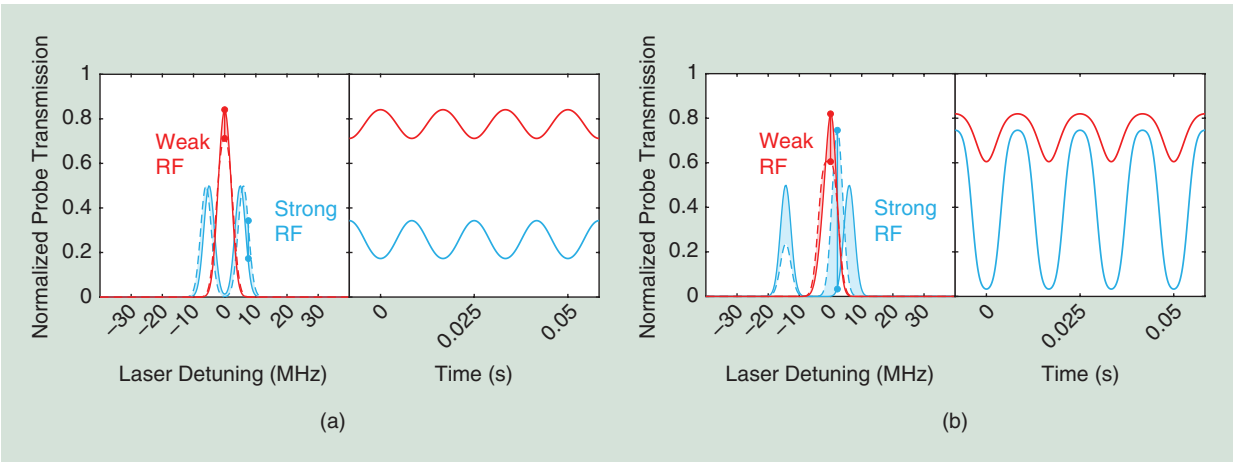

Figure 10. *A simulated Rydberg atom sensor signal (for a given set of states and optical powers) when detecting (a) AM (60 Hz) and (b) FM (60 Hz) RF signals. When the RF field is strong enough to induce AT splitting, the probe (or coupling) laser is locked to an off-resonance frequency corresponding to a point of large change in probe transmission, as indicated by the large dots. Otherwise, the optimal point for obtaining the largest probe transmission signal is on resonance.*

Not only can we measure the strength of an incident RF E-field with atom-based sensors, we can also detect the phase and tune the polarization response.

QAM signals with a high number of bases were transmitted, the error rates increase for lower symbol rates. This is due to the crowding of the phase states while also extracting amplitude information, and it limits the symbol rate that can be received. This work marks the beginning of important studies of the capabilities and limitations of Rydberg sensors for communications applications. Improving the sensitivity of these devices and reducing the noise within the detection of communications signals (see the "Pushing the Boundaries of Sensitivity and Bandwidth" section) is an active area of research that will have a significant impact on the bit error rates achievable with future Rydberg sensors.

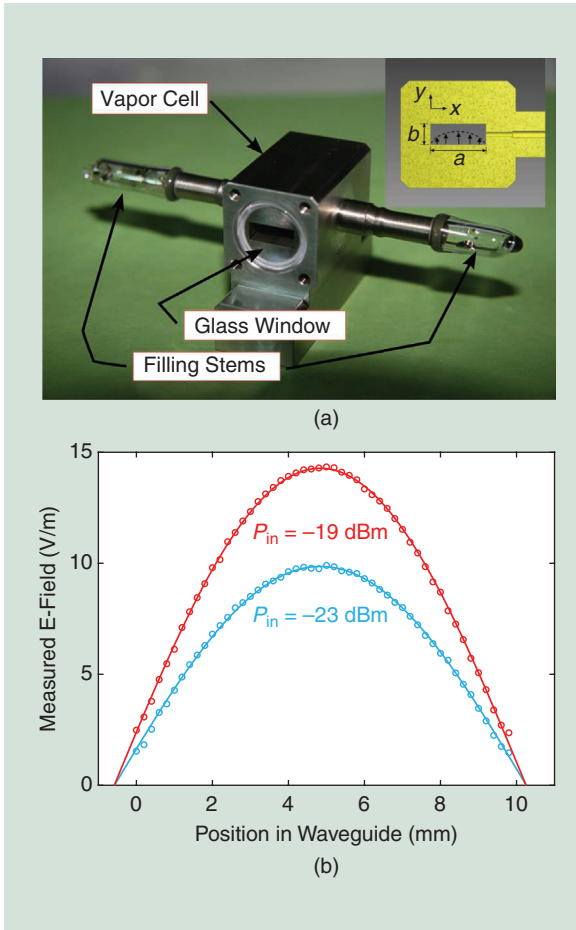

Figure 11. *(a) The Rydberg atom waveguide vapor cell. The inset shows the distribution of the E-field across the x-axis. (Source: [44, Fig. 1]; used with permission.) (b) The E-field atom measurement by scanning the lasers within the waveguide while varying the input RF power [44]. dBm: decibels relative to 1 mW.*

Extending Field Measurements to Voltage and Power

Building from field measurements with Rydberg atom sensors, we can apply field confinement ideas to measure properties such as voltage and power. These measurements are governed by the geometric confinement of the field in a knowable way. In the case of power, Rydberg sensors are embedded in a rectangular waveguide for in situ RF power calibration (see Figure 11 [44]). Unlike traditional RF power meters, Rydberg atom waveguide power meters do not absorb RF radiation, instead leaving it for immediate use as a calibrated source in a desired application. Using Rydberg atoms for voltage measurements has the potential to be an alternative calibration instrument to the precise but expensive Josephson voltage standard and the less accurate but cost-effective Zener diodes [45]. Rydberg atom-based voltage measurement systems are expected to fit between these two technologies as an option that is more accurate than Zener diodes and less expensive than the Josephson voltage standard.

RF power calibrations are essential for many electronic systems, including radar and advanced communications technologies. Many of these systems require repeat calibrations of the RF sources that consume resources and operation time. By leveraging knowledge of the E-field mode in a rectangular waveguide, Holloway et al. demonstrated the use of Rydberg cesium atoms to measure RF power in waveguides [44]. They first mapped out the distribution of field strength within the waveguide by shifting the position of the lasers with respect to the waveguide cross section to determine the location of the maximum field amplitude, for example, Figure 11(b). Then, the RF power within the waveguide was simply given by this peak field amplitude and a set of geometric parameters defining the dimensions of the rectangular waveguide. The resulting power meter leverages the absolute field measurements of Rydberg atom sensors and has the especially unique characteristic of being a fully in situ measurement of RF power because, unlike calorimeters and diodes, RF radiation is not absorbed by the Rydberg atom device. Without the absorption of the RF field, the radiation is immediately available for its intended application and carries with it a real-time, absolute measure of the total power in a waveguide. The Rydberg power meter also has all the benefits of the standard Rydberg E-field sensor, including good sensitivity and dynamic range, low uncertainty, and a large frequency range of operation.

Most of the systems described in this article apply the EIT/AT technique, the splitting of the narrow EIT

line of the probe laser transmission by coherent interference between Rydberg states and modifications thereof, such as the atom mixer. The detection of voltage potential between parallel plates, on the other hand, employs the Stark shift effect, where the EIT line shifts in frequency in the probe transmission spectrum. Stark shifts are an off-resonance effect, which means dc and quasi-dc (60-Hz) signals can be detected with Rydberg atoms [45]. This Stark frequency shift is proportional to the square of the E-field between plates times the polarizability of the atoms—another calculable constant of the atoms and the state they are driven to. We start by sealing two parallel plates in the vapor cell, as pictured in Figure 12(a). Once we calibrate the spacing between the plates, we can decipher the voltage potential between them from a measurement of the E-field via the Stark shift effect [Figure 12(b)]. This effect can be enhanced by combining the dc field measurement with an RF dressing of the Rydberg state, as described by Bason et al. [46]. The parallel plates can also be fabricated as thin films on the walls of the vapor cell, as implemented by Daschner et al. [47], [48]. Field inhomogeneities are the primary culprit of line broadening and give rise to reduced detection resolution, especially as the field strength is increased. These inhomogeneities can be caused by the ionization of the atoms by the high-energy visible laser [48], and they may arise from fringe fields at the boundaries of the parallel plates as well as the divergence of the plates from parallelity [45].

Resolving the Angle of Arrival and Forming Images

One particular trait of Rydberg atom sensors is the ease of achieving an exceptionally small sensing area. The sensitive region of these devices is defined by the overlapping volume of the lasers. The laser beamwidth is commonly submillimeter, making the active region of the E-field sensor subwavelength along this dimension relative to an incident RF field. An early demonstration using the subwavelength nature of the atomic probes was completed by Holloway et al. in 2014, where the probe and coupling lasers were scanned across the diameter of a cylindrical vapor cell [12]. This measurement showed the variation in field amplitude within the vapor cell due to internal reflections of the RF field between the glass walls of the cell. This measurement highlights the importance of understanding, and calibrating when necessary, the effect of the vapor cell on absolute measurements of an RF field. Modifying the vapor cell architecture to eliminate internal reflections of the RF field is an active area of research.

By feeding the lasers to a small vapor cell via optical fiber coupling, the mapping of E-fields radiating from various devices and propagating through a space is easily achieved. For example, measurements of the field distribution above a coplanar waveguide, measurements above a transverse electromagnetic cell aperture, measurements within a gigahertz transverse electromagnetic cell showing frequency-dependent field variation as a function of position within the cell, and the gain pattern of a horn antenna have all been demonstrated [7], [10], [49]. The imaging of the near-field distribution radiated by a Yagi–Uda antenna with uncertainties below 5.5% was also demonstrated using Rydberg atom sensors [50]. The uncertainty of these measurements was dominated by the positioning of the Rydberg sensor and still achieved an improvement over traditional methods.

More recently, early demonstrations of a fiber-coupled Rydberg sensor used for synthetic aperture measurements in channel sounding applications have been put forward [51]. In all these applications, the Rydberg sensor has the unique benefit of being minimally perturbative to the RF field under investigation. The weak scattering of the RF radiation by the dielectric vapor cell is especially valuable in channel measurements, where the scattering of the field off the receiver often leads to multiple reflections within the channel that

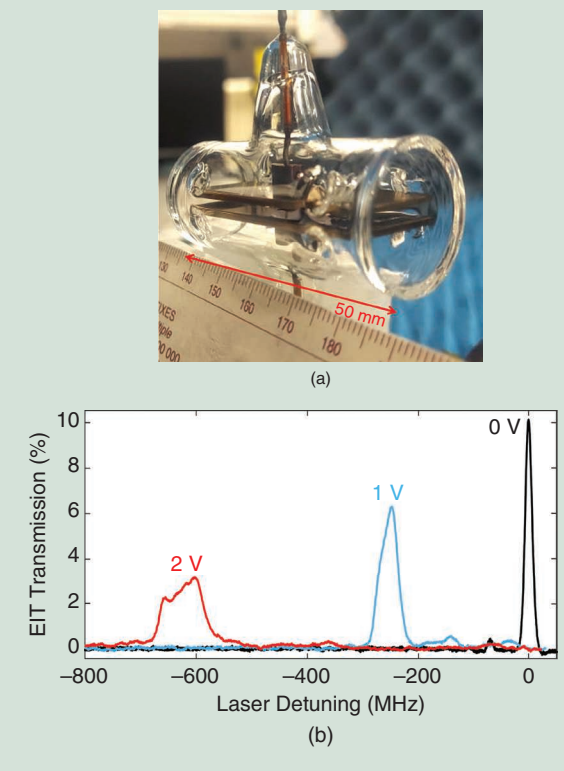

Figure 12. *(a) The vapor cell used by Holloway et al. for voltage reference measurements. (b) The measured frequency shift of the EIT line when the voltage potential between parallel plate electrodes is increased.*

It is quite amazing that during this time, we have learned to control ensembles of atoms to such an extent that various unique applications are starting to emerge.

are ultimately measured as additional scatterers and sources in the environment. The next advance in this space will likely be arrays of Rydberg atom sensors. Such devices have been proposed as RF field imagers [52]–[56].

Coherently combining multiple spatial measurements of an RF field while measuring the phase of the field (either by the mixer/heterodyne method or the all-optical method) enables a measurement of the angle of arrival (AoA) of the RF radiation. To determine the AoA, a phase difference is measured between two spatial locations. In far-field measurements where the RF wavefront is planar, the sine of the AoA is directly related to the measured phase difference. Such measurements were completed by Robinson et al., wherein two spatially separated phase measurements were simultaneously captured by passing two sets of lasers through a single vapor cell [57]. Figure 13 depicts the setup of this AoA measurement demonstration.

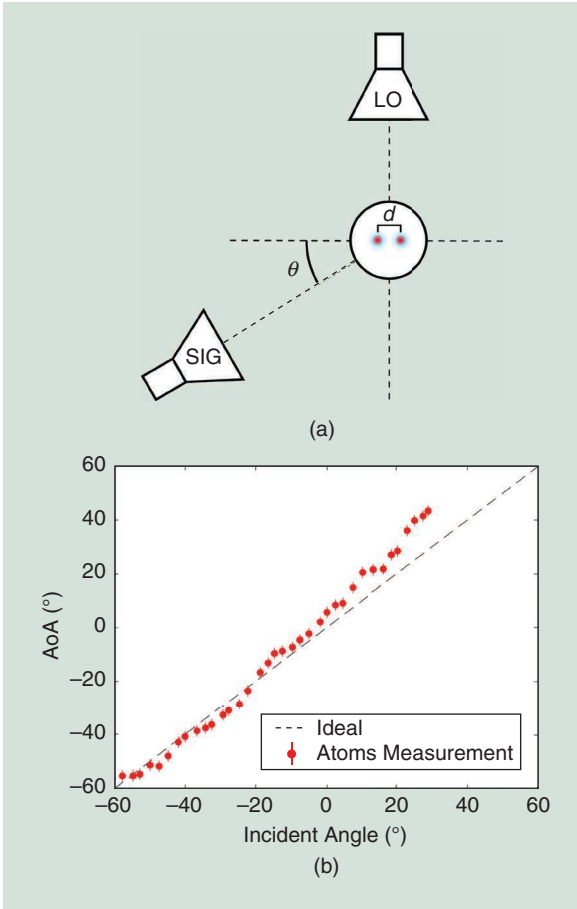

Figure 13. *(a) The experimental setup for demonstrating the measurement of an RF signal (SIG) AoA (θ) with a cylindrical vapor cell and two sets of optical lasers separated by a space d along the orthogonal axis to the LO propagation axis. (b) A comparison of expected and measured AoAs. (Source: [57]; used with permission.)*

RF field imagers, or arrays of Rydberg atom sensors, are expected to have the ability to detect subwavelength spatial images of the RF E-field magnitude and phase and may improve signal polarimetry in radar systems [54]. Other work has shown that by sampling the phase of an incident RF field at various locations in a vapor cell, one can characterize other aspects of an RF source and increase its data capacity [58]. Finally, Rydberg atom sensors have been shown to be useful as a noninvasive method of measuring and characterizing plasmas [59], for possible black-body thermometry [60], and for waveform detection and spectrum analyzers [31], [51].

Where Modern Field Measurements With Atoms Are Going

There has been great progress in the development of Rydberg atom-based sensors over the past 10 years. It is quite amazing that during this time, we have learned to control ensembles of atoms to such an extent that various unique applications are starting to emerge. Because of the numerous potential applications, several groups around the world have begun programs in the area of Rydberg atom-based sensors/receivers, including universities, private companies, government agencies, and most national metrology institutes.

Some areas of research that are generating the most excitement include pushing the boundaries of sensitivity to the single-nV/cm$\sqrt{\text{Hz}}$ level (an order of magnitude better than the current best) while maintaining a high saturation cutoff of strong RF fields, for example, the detectability of near-kilovolt/centimeter field strengths. Widening the dynamic range of sensitivity of these sensors will have a significant impact on all applications using Rydberg atoms to detect E-fields. In particular, some frequency bands are more challenging to detect with low sensitivity than others. The location of GPS signals and the like will require improvements to both sensitivity and data detection rates. Boosting data rates to the near-gigabit/second level is another major interest of groups using these devices for a wide swath of communications applications. Furthermore, improvements to the precision and accuracy of AoA measurements, i.e., coherent phase sensitivity better than 1° across a spatial plane of interest, along with implementations of subwavelength Rydberg arrays will support the application

of Rydberg atom sensors in the context of imaging, metrology, and reconnaissance.

Rydberg systems that employ the the ladder scheme depicted in Figure 2 rely on single-frequency, tunable visible lasers (the coupling laser) to reach Rydberg atomic states. These systems are bulky and expensive and limit both the portability of Rydberg atom sensors and the scalability of these devices, due to the costs associated with the coupling laser. Many teams are therefore pursuing architectures that utilize multiple lasers at more easily available wavelengths in place of a single visible laser to reach Rydberg states, and technological advances to shrink the size and cost of the blue and green coupling lasers are being developed in parallel. Commercial room temperature Rydberg atom sensors are just starting to appear [61], [62]. Over the next few years, commercial Rydberg sensors are likely to become increasingly available as interest in these devices increases, helping to reduce costs.

Meanwhile, in metrology and academic labs around the world, researchers are studying uncertainties in these E-field measurements, resolving how to increase the absolute accuracy of the devices, and verifying the precision with which field strength is measured. Across-the-board testing and characterization of these new sensors/receivers is needed to determine where the devices can offer the best improvement over traditional classical systems and where a combination of the two paradigms is beneficial. Anticipated progress in advancing and improving Rydberg atom sensors will lead to powerful devices for the wideband, often metal-free detection of RF E-fields, communications signals, dc and ac voltage, real-time power, wavefronts, and much more.

References

[1] J. D. Kraus, "Heinrich hertz-theorist and experimenter," *IEEE Trans. Microw. Theory Techn.*, vol. 36, no. 5, pp. 824–829, 1988, doi: 10.1109/22.3601.

[2] P. K. Bondyopadhyay, "Guglielmo Marconi - The father of long distance radio communication - An engineer's tribute," in *Proc. 1995 25th Eur. Microw. Conf.*, vol. 2, pp. 879–885, doi: 10.1109/EUMA.1995.337090.

[3] D. B. Newell *et al.*, "The CODATA 2017 values of h, e, k, and N_A for the revision of the SI," *Metrologia*, vol. 55, no. 1, pp. L13–L16, Jan. 2018, doi: 10.1088/1681-7575/aa950a.

[4] M. Stock, "The revision of the SI – Towards an international system of units based on defining constants," *Meas. Techn.*, vol. 60, no. 12, pp. 1169–1177, 2018, doi: 10.1007/s11018-018-1336-2.

[5] J. A. Gordon, C. L. Holloway, S. Jefferts, and T. Heavner, "Quantum-based SI traceable electric-field probe," in *Proc. 2010 IEEE Int. Symp. Electromagn. Compat.*, pp. 321–324, doi: 10.1109/ISEMC.2010.5711293.

[6] J. A. Sedlacek, A. Schwettmann, H. Kübler, R. Löw, T. Pfau, and J. P. Shaffer, "Microwave electrometry with Rydberg atoms in a vapour cell using bright atomic resonances," *Nature Phys.*, vol. 8, no. 11, pp. 819–824, Nov. 2012, doi: 10.1038/nphys2423.

[7] M. T. Simons, J. A. Gordon, and C. L. Holloway, "Fiber-coupled vapor cell for a portable Rydberg atom-based radio frequency electric field sensor," *Appl. Opt.*, vol. 57, no. 22, pp. 6456–6460, Aug. 2018, doi: 10.1364/AO.57.006456.

[8] T. F. Gallagher, *Rydberg Atoms* (Cambridge Monographs on Atomic, Molecular and Chemical Physics Series). Cambridge, U.K.: Cambridge Univ. Press, 1994.

[9] C. L. Holloway *et al.*, "Broadband Rydberg atom-based electric-field probe for SI-traceable, self-calibrated measurements," *IEEE Trans. Antennas Propag.*, vol. 62, no. 12, pp. 6169–6182, 2014, doi: 10.1109/TAP.2014.2360208.

[10] C. L. Holloway *et al.*, "Atom-based RF electric field metrology: From self-calibrated measurements to subwavelength and near-field imaging," *IEEE Trans. Electromagn. Compat.*, vol. 59, no. 2, pp. 717–728, 2017, doi: 10.1109/TEMC.2016.2644616.

[11] J. A. Gordon *et al.*, "Millimeter wave detection via Autler-Townes splitting in rubidium Rydberg atoms," *Appl. Phys. Lett.*, vol. 105, no. 2, p. 024104, 2014, doi: 10.1063/1.4890094.

[12] C. L. Holloway *et al.*, "Sub-wavelength imaging and field mapping via electromagnetically induced transparency and Autler-Townes splitting in Rydberg atoms," *Appl. Phys. Lett.*, vol. 104, no. 24, p. 244,102, 2014, doi: 10.1063/1.4883635.

[13] K.-J. Boller, A. Imamoğlu, and S. E. Harris, "Observation of electromagnetically induced transparency," *Phys. Rev. Lett.*, vol. 66, no. 20, pp. 2593–2596, May 1991, doi: 10.1103/PhysRevLett.66.2593.

[14] A. K. Mohapatra, T. R. Jackson, and C. S. Adams, "Coherent optical detection of highly excited Rydberg states using electromagnetically induced transparency," *Phys. Rev. Lett.*, vol. 98, no. 11, p. 113,003, Mar. 2007, doi: 10.1103/PhysRevLett.98.113003.

[15] C. L. Holloway, M. T. Simons, J. A. Gordon, A. Dienstfrey, D. A. Anderson, and G. Raithel, "Electric field metrology for SI traceability: Systematic measurement uncertainties in electromagnetically induced transparency in atomic vapor," *J. Appl. Phys.*, vol. 121, no. 23, p. 233,106, 2017, doi: 10.1063/1.4984201.

[16] M. T. Simons, M. D. Kautz, J. A. Gordon, and C. L. Holloway, "Uncertainties in Rydberg atom-based RF e-field measurements," in *Proc. 2018 Int. Symp. Electromagn. Compat. (EMC EUROPE)*, pp. 376–380, doi: 10.1109/EMCEurope.2018.8485055.

[17] H. Fan, S. Kumar, J. Sheng, J. P. Shaffer, C. L. Holloway, and J. A. Gordon, "Effect of vapor-cell geometry on Rydberg-atom-based measurements of radio-frequency electric fields," *Phys. Rev. Appl.*, vol. 4, no. 4, p. 044015, Oct. 2015, doi: 10.1103/PhysRevApplied.4.044015.

[18] M. T. Simons, J. A. Gordon, and C. L. Holloway, "Simultaneous use of cs and RB Rydberg atoms for dipole moment assessment and RF electric field measurements via electromagnetically induced transparency," *J. Appl. Phys.*, vol. 120, no. 12, p. 123,103, 2016, doi: 10.1063/1.4963106.

[19] J. A. Gordon, M. T. Simons, A. H. Haddab, and C. L. Holloway, "Weak electric-field detection with sub-1 Hz resolution at radio frequencies using a Rydberg atom-based mixer," *AIP Adv.*, vol. 9, no. 4, p. 045030, 2019, doi: 10.1063/1.5095633.

[20] D. A. Anderson *et al.*, "Two-photon microwave transitions and strong-field effects in a room-temperature Rydberg-atom gas," *Phys. Rev. A*, vol. 90, no. 4, p. 043419, Oct. 2014, doi: 10.1103/PhysRevA.90.043419.

[21] D. A. Anderson, S. A. Miller, G. Raithel, J. A. Gordon, M. L. Butler, and C. L. Holloway, "Optical measurements of strong microwave fields with Rydberg atoms in a vapor cell," *Phys. Rev. Appl.*, vol. 5, no. 3, p. 034003, Mar. 2016, doi: 10.1103/PhysRevApplied.5.034003.

[22] H. Friedrich, *Theoretical Atomic Physics* (Springer Series in Computational Series). Park Ridge, NJ, USA: Noyes, 1991.

[23] J. A. Sedlacek, A. Schwettmann, H. Kübler, and J. P. Shaffer, "Atom-based vector microwave electrometry using rubidium Rydberg atoms in a vapor cell," *Phys. Rev. Lett.*, vol. 111, no. 6, p. 063001, Aug. 2013, doi: 10.1103/PhysRevLett.111.063001.

[24] D. A. Anderson, E. G. Paradis, and G. Raithel, "A vapor-cell atomic sensor for radio-frequency field detection using a polarization-selective field enhancement resonator," *Appl. Phys. Lett.*, vol. 113, no. 7, p. 073501, 2018, doi: 10.1063/1.5038550.

[25] M. T. Simons, A. H. Haddab, J. A. Gordon, D. Novotny, and C. L. Holloway, "Embedding a Rydberg atom-based sensor into an antenna for phase and amplitude detection of radio-frequency fields

and modulated signals," *IEEE Access*, vol. 7, pp. 164,975–164,985, Oct. 2019, doi: 10.1109/ACCESS.2019.2949017.

[26] M. T. Simons, A. H. Haddab, J. A. Gordon, and C. L. Holloway, "A Rydberg atom-based mixer: Measuring the phase of a radio frequency wave," *Appl. Phys. Lett.*, vol. 114, no. 11, p. 114,101, 2019, doi: 10.1063/1.5088821.

[27] M. Jing *et al.*, "Atomic superheterodyne receiver based on microwave-dressed Rydberg spectroscopy," *Nature Phys.*, vol. 16, no. 9, pp. 911–915, Jun. 2020, doi: 10.1038/s41567-020-0918-5.

[28] D. A. Anderson, R. E. Sapiro, and G. Raithel, "Rydberg atoms for radio-frequency communications and sensing: Atomic receivers for pulsed RF field and phase detection," *IEEE Aerosp. Electron. Syst. Mag.*, vol. 35, no. 4, pp. 48–56, 2020, doi: 10.1109/MAES.2019.2960922.

[29] D. A. Anderson, R. E. Sapiro, L. F. Gonçalves, R. Cardman, and G. Raithel, "Atom radio-frequency interferometry," 2010, arXiv:2010.13657.

[30] S. Kumar, H. Fan, H. Kübler, J. Sheng, and J. P. Shaffer, "Atom-based sensing of weak radio frequency electric fields using homodyne readout," *Scientific Rep.*, vol. 7, no. 1, p. 42,981, Feb. 2017, doi: 10.1038/srep42981.

[31] D. H. Meyer, P. D. Kunz, and K. C. Cox, "Waveguide-coupled Rydberg spectrum analyzer from 0 to 20 GHz," *Phys. Rev. Appl.*, vol. 15, no. 1, p. 014053, Jan. 2021, doi: 10.1103/PhysRevApplied.15.014053.

[32] N. Prajapati, A. K. Robinson, S. Berweger, M. T. Simons, A. B. Artusio-Glimpse, and C. L. Holloway, "Enhancement of electromagnetically induced transparency based Rydberg-atom electrometry through population repumping," *Appl. Phys. Lett.*, vol. 119, no. 21, p. 214,001, 2021, doi: 10.1063/5.0069195.

[33] M. T. Simons *et al.*, "Continuous radio-frequency electric-field detection through adjacent Rydberg resonance tuning," *Phys. Rev. A*, vol. 104, no. 3, p. 032824, Sep. 2021, doi: 10.1103/PhysRevA.104.032824.

[34] C. Holloway *et al.*, "A multiple-band Rydberg atom-based receiver: AM/FM stereo reception," *IEEE Antennas Propag. Mag.*, vol. 63, no. 3, pp. 63–76, 2021, doi: 10.1109/MAP.2020.2976914.

[35] A. B. Deb and N. Kjærgaard, "Radio-over-fiber using an optical antenna based on Rydberg states of atoms," *Appl. Phys. Lett.*, vol. 112, no. 21, p. 211,106, 2018, doi: 10.1063/1.5031033.

[36] D. H. Meyer, K. C. Cox, F. K. Fatemi, and P. D. Kunz, "Digital communication with Rydberg atoms and amplitude-modulated microwave fields," *Appl. Phys. Lett.*, vol. 112, no. 21, p. 211,108, 2018, doi: 10.1063/1.5028357.

[37] K. C. Cox, D. H. Meyer, F. K. Fatemi, and P. D. Kunz, "Quantum-limited atomic receiver in the electrically small regime," *Phys. Rev. Lett.*, vol. 121, no. 11, p. 110,502, Sep. 2018, doi: 10.1103/PhysRevLett.121.110502.

[38] Z. Song *et al.*, "Rydberg-atom-based digital communication using a continuously tunable radio-frequency carrier," *Opt. Exp.*, vol. 27, no. 6, pp. 8848–8857, Mar. 2019, doi: 10.1364/OE.27.008848.

[39] D. A. Anderson, R. E. Sapiro, and G. Raithel, "An atomic receiver for AM and FM radio communication," *IEEE Trans. Antennas Propag.*, vol. 69, no. 5, pp. 2455–2462, 2021, doi: 10.1109/TAP.2020.2987112.

[40] C. L. Holloway, M. T. Simons, A. H. Haddab, C. J. Williams, and M. W. Holloway, "A 'real-time' guitar recording using Rydberg atoms and electromagnetically induced transparency: Quantum physics meets music," *AIP Adv.*, vol. 9, no. 6, p. 065110, 2019, doi: 10.1063/1.5099036.

[41] M. T. Simons *et al.*, "Electromagnetically induced transparency (EIT) and Autler-Townes (AT) splitting in the presence of band-limited white gaussian noise," *J. Appl. Phys.*, vol. 123, no. 20, p. 203,105, 2018, doi: 10.1063/1.5020173.

[42] C. L. Holloway, M. T. Simons, J. A. Gordon, and D. Novotny, "Detecting and receiving phase-modulated signals with a Rydberg atom-based receiver," *IEEE Antennas Wireless Propag. Lett.*, vol. 18, no. 9, pp. 1853–1857, 2019, doi: 10.1109/LAWP.2019.2931450.

[43] J. S. Otto, M. K. Hunter, N. Kjærgaard, and A. B. Deb, "Data capacity scaling of a distributed Rydberg atomic receiver array," *J. Appl. Phys.*, vol. 129, no. 15, p. 154,503, 2021, doi: 10.1063/5.0048415.

[44] C. L. Holloway, M. T. Simons, M. D. Kautz, A. H. Haddab, J. A. Gordon, and T. P. Crowley, "A quantum-based power standard: Using Rydberg atoms for a SI-traceable radio-frequency power measurement technique in rectangular waveguides," *Appl. Phys. Lett.*, vol. 113, no. 9, p. 094101, 2018, doi: 10.1063/1.5045212.

[45] C. L. Holloway *et al.*, "Electromagnetically induced transparency based Rydberg-atom sensor for quantum-based voltage measurements," 2021, arXiv:2110.02335v1.

[46] M. G. Bason *et al.*, "Enhanced electric field sensitivity of RF-dressed Rydberg dark states," *New J. Phys.*, vol. 12, no. 6, p. 065015, Jun. 2010, doi: 10.1088/1367-2630/12/6/065015.

[47] R. Daschner *et al.*, "Fabrication and characterization of an electrically contacted vapor cell," *Opt. Lett.*, vol. 37, no. 12, pp. 2271–2273, Jun. 2012, doi: 10.1364/OL.37.002271.

[48] R. Daschner, H. Kübler, R. Löw, H. Baur, N. Frühauf, and T. Pfau, "Triple stack glass-to-glass anodic bonding for optogalvanic spectroscopy cells with electrical feedthroughs," *Appl. Phys. Lett.*, vol. 105, no. 4, p. 041107, 2014, doi: 10.1063/1.4891534.

[49] C. L. Holloway, M. T. Simons, M. Kautz, P. F. Wilson, and J. A. Gordon, "Development and applications of a fiber-coupled atom-based electric field probe," in *Proc. 2018 Int. Symp. Electromagn. Compat. (EMC EUROPE)*, pp. 381–385, doi: 10.1109/EMCEurope.2018.8485006.

[50] R. Cardman, L. F. Gonçalves, R. E. Sapiro, G. Raithel, and D. A. Anderson, "Atomic 2D electric field imaging of a Yagi-UDA antenna near-field using a portable Rydberg-atom probe and measurement instrument," *Adv. Opt. Technol.*, vol. 9, no. 5, pp. 305–312, Nov. 2020, doi: 10.1515/aot-2020-0029.

[51] M. T. Simons, A. B. Artusio-Glimpse, A. K. Robinson, N. Prajapati, and C. L. Holloway, "Rydberg atom-based sensors for radio-frequency electric field metrology, sensing, and communications," *Meas., Sensors*, vol. 18, p. 100,273, Dec. 2021, doi: 10.1016/j.measen.2021.100273.

[52] H. Amarloo, J. Ramirez-Serrano, and J. P. Shaffer, "Vapor cells for imaging of electromagnetic fields," U.S. Patent Grant 11 112 298, 2020.

[53] H. Amarloo, J. Ramirez-Serrano, and J. P. Shaffer, "Photonic-crystal vapor cells for imaging of electromagnetic fields," U.S. Patent Appl. 17/308,588, 2020.

[54] H. Amarloo, J. Ramirez-Serrano, and J. P. Shaffer, "Radar systems using photonic crystal receivers to detect target objects," U.S. Patent Appl. 17/201,830, 2021.

[55] V. Aksyuk, C. Holloway, A. Artusio-Glimpse, and M. Simons, "Photonic Rydberg atom radio frequency sensor array," U.S. Patent Appl. 63/228,238, 2021.

[56] C. L. Holloway, J. Kitching, A. Artusio-Glimpse, V. Aksyuk, M. T. Simons, and O. D. Lopez, "Atomic vapor cell and making an atomic vapor cell," U.S. Patent Appl. 17/374,537, 2021.

[57] A. K. Robinson, N. Prajapati, D. Senic, M. T. Simons, and C. L. Holloway, "Determining the angle-of-arrival of a radio-frequency source with a Rydberg atom-based sensor," *Appl. Phys. Lett.*, vol. 118, no. 11, p. 114,001, 2021, doi: 10.1063/5.0045601.

[58] S. Ottoa, M. Hunter, N. Kjærgaard, and A. Debb, "Data capacity scaling of a distributed Rydberg atomic receiver array," *J. Appl. Phys.*, vol. 129, no. 15, p. 154,503, 2021, doi: 10.1063/5.0048415.

[59] D. Anderson, G. Raithel, M. Simons, and C. Holloway, "Quantum-optical spectroscopy for plasma electric field measurements and diagnostics," Dec. 23, 2017, arXiv:1712.08717v1.

[60] E. Norrgard, S. Eckel, C. Holloway, and E. Shirley, "Quantum blackbody thermometry," *New J. Phys.*, vol. 23, no. 3, p. 033037, 2021, doi: 10.1088/1367-2630/abe8f5.

[61] "Rydberg technologies: Quantum sensing and measurement solutions," Rydberg Technologies Inc., Ann Arbor, MI, USA, 2020. [Online]. Available: http://www.rydbergtechnologies.com/

[62] D. A. Anderson, R. E. Sapiro, and G. Raithel, "A self-calibrated SI-traceable Rydberg atom-based radio frequency electric field probe and measurement instrument," *IEEE Trans. Antennas Propag.*, vol. 69, no. 9, pp. 5931–5941, Sep. 2021, doi: 10.1109/TAP.2021.3060540.

[63] C. S. Adams *et al.*, "Rydberg atom quantum technologies," *J. Phys. B: At. Mol. Opt. Phys.*, vol. 53, 2020, Art. no. 012002. [Online]. Available: https://doi.org/10.1088/1361-6455/ab52ef